Low-cycle fatigue behavior of glass-fiber-reinforced polymers cross arms with steel sleeves

Low-cycle fatigue behavior of glass-fiber-reinforced polymers cross arms with steel sleeves

H B Sun[1], Q Sun[2], S J Zhang[1], Y L Peng[1] and J T Wang[2,*]

[1]Henan Electric Power Survey & Design Institute, West Zhongyuan Road No. 212, 450007, Zhengzhou, Henan Province, China
[2]Department of Civil Engineering, Xi'an Jiaotong University, West Xianning Road No. 28, 710049, Xi'an, Shaanxi Province, China

Corresponding author and e-mail: J T Wang, wangjiantao@stu.xjtu.edu.cn

Abstract. For the dynamic fatigue problem of transmission tower cross arms caused by the strong wind load, an experimental study on low-cycle fatigue behavior of a new type full-scale glass-fiber-reinforced polymers (GFRP) cross arm with steel sleeves was carried out. A total of six specimens were subjected to cyclic loading for simulating low-cycle fatigue. The stress state was monitored. The variety of load-displacement-time curve, energy dissipation and dynamic strain were analyzed. The ultimate bearing capacity of the specimens without significant fatigue failure was examined to derive residual bearing capacity. Based on the residual strength theory, the cumulative damage was evaluated to predict the fatigue life. It is shown that the GFRP cross arms demonstrated favourable anti-fatigue performance, and can be expected to provide important reference for wind resistance design in transmission tower line system.

1. Introduction

Glass-fiber-reinforced polymers (GFRP) has been applied in power transmission engineering widely as a replacement of conventional materials (wood, concrete and steel) due to its unique advantages of high strength-to-weight ratio, resistance to corrosion, lower transportation and maintenance costs. Adopting composite material cross arms in transmission tower can improve the reliability of power supplication by reducing the adverse effects of partial discharge and contamination flashover, while it can bring significant economic benefits through narrowing the width of transmission line corridor and maintenance costs [1]. However, owing to the lofty-soft feature and strong geometrical nonlinearity of transmission tower line coupling system, which is sensitive to external wind excitation, especially under strong dynamic wind loads (typhoons, thunderstorms), the powerful wind-induced vibration response of the coupling system can lead to the dynamic instability and fatigue failure of the local components, and finally result in the overall collapse phenomenon [2].

Cross arms, as an important component connecting transmission towers and transmission lines, are exposed to complex stress condition. The low-cycle fatigue load of cross arm caused by strong wind with small recurrence frequencies and large amplitudes, is a safety problem that cannot be neglected in the design period [3]. During the past decades, great contributions have been done to investigate the fatigue behavior of composite materials [4-11]. However, the aforementioned studies mainly focus on cumulative damage assessment and fatigue life prediction based on materials level, and the studies on

low-cycle behavior of full-scale GFRP cross arms with steel sleeves were found lacking. For the low-fatigue behavior induced by strong wind, further experimental investigation on low-cycle fatigue behavior of GFRP cross arms should be carried out for better engineering application.

In this paper, a total of six specimens were subjected to low-cycle loading to investigate the fatigue behavior. The ultimate bearing capacity of the specimens without significant fatigue failure was examined to derive residual bearing capacity. Based on the modified residual strength theory at component level, the cumulative damage was evaluated and to predict the fatigue life. The experimental research in this paper could provide significant references to wind resistance design.

2. Experimental conditions

2.1. Specimen details

A total of six specimens were tested to examine the low-cycle fatigue behavior. The specimen size and arrangement of measuring points are shown in Figure 1.

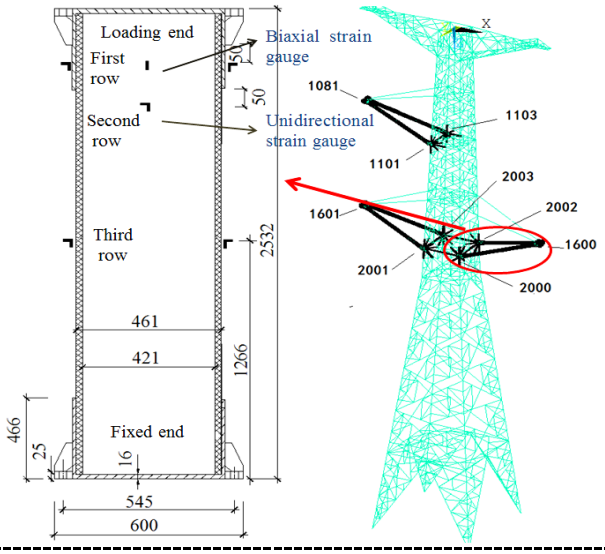

Figure 1. Specimen size and arrangement of measuring points.

As shown in Figure 1, the composite cross arm was 2532 mm long and the length of Q345 steel casing was 466 mm. The outer diameter and wall thickness of the GFRP pipe were 461 mm and 20 mm, respectively. The wall thickness and outer diameter of steel casing, with 16 stiffening ribs along the perimeter, were 16 mm 600 mm, respectively. The strain gauges were mainly mounted on the loading end, which was sensitive to fatigue loads. Four biaxial and unidirectional strain gauges of the first row were arranged in an interval of 90° along the circumferential direction; two strain gauges of the second or the third row were set up in symmetrical layout.

2.2. Loading scheme

In this paper, based on the Ximeng-Shengli section ultra- high voltage (UHV) transmission project in China, the finite element method was utilized to conduct dynamic time-history analysis for determining fatigue peak loads of experiment. The internal force of the transmission tower cross arms at the strong wind speed of 30 m/s was extracted as the ultimate reference condition. Based on the local climatic condition, 3500 cycles loading were determined to simulate the actual stress state. The fatigue test was carried out by MTS244.51 hydraulic servo actuation system. The loading scheme is shown in Table 1.

As shown in Table 1, the fatigue cycle load was applied through the displacement control mode. After the test, the ultimate bearing capacity of the specimens without significant fatigue failure was evaluated to derive residual bearing capacity using 20000kN computer controlled electro-hydraulic servo pressure machine to evaluate the fatigue damage. The loading device of low-cycle fatigue test and residual ultimate bearing capacity test are shown in Figure 2 and Figure 3, respectively.

Table 1. Loading protocol.

specimen	Loading condition	Loads peak(kN)		Cycles	Frequency (Hz)	comments
		Upper limit (compression)	Lower limit (tension)			
DZ-1	1	179.00	-41.00	3500	0.5	Speed: 30 m/s
DZ-2	2	358.00	-82.00	3500	0.5	/
DZ-3	3	720.00	-360.00	3500	0.5	/
DZ-4	4	-90.00	-900.00	3500	0.25	/
DZ-5	5	720.00	-720.00	3500	0.25	/
DZ-6	6	900.00	-900.00	3500	0.25	/

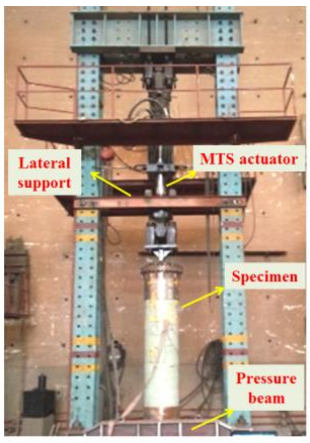

Figure 2. Low-cycle fatigue test.

Figure 3. Residual bearing capacity test.

3. Test results and analysis

3.1. Summary of test result

Table 2. Summary of the test result.

Specimen	Test phenomenon
DZ-1	No significant fatigue failure phenomenon
DZ-2	Making slight sound during every loading cycle, there is no visible fatigue failure after test.
DZ-3	Producing clear sound firstly and then to slight, no significant fatigue failure appears finally.
DZ-4	Making slight sound during every loading cycle, there is no visible fatigue failure after test.
DZ-5	Producing clear sound during every loading cycle, no significantly visible fatigue failure occurs finally.
DZ-6	Producing clear sound during every loading cycle, no significantly visible fatigue failure occurs finally.

After the low-cycle fatigue test, the summary of test results is shown in Table 2. No obvious fatigue failure phenomenon was observed during the test. In order to guarantee the maximum safety margin and to evaluate the cumulative damage, the axial compression test was carried out to derive the residual ultimate bearing capacity of DZ-5 and DZ-6 based on the worst loading condition. The final failure type was that shear failure appeared in composite material portion. The typical failure mode is shown in Figure 4. It indicated that the ultimate bearing capacity was reached as the layered fibers broke from the resin accompanied by a huge 'bang' heard simultaneously.

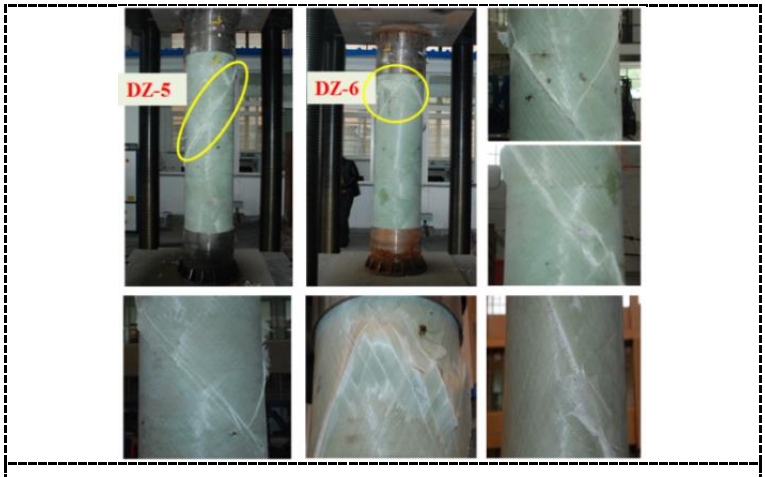

Figure 4. Typical shear failure.

3.2. Load-displacement-time curves

The variety of mechanical properties of GFRP cross arms can be monitored by load-displacement-time curves during the fatigue test. The DZ-6 specimen under the loading condition 6 was taken as an example to illustrate the whole load-displacement-time curve. The load-displacement-time curve of DZ-6 specimen is shown in Figure 5. It could be seen that the load peak and valley of the specimen were stable during the fatigue test, which was consistent with the expectant value of the loading scheme. Compared with the load-displacement-time curve analysis and test results of the other specimens, it is shown that the GFRP cross arm specimens have good workability after 3,500 times of low-cycle fatigue loading without obvious fatigue failure phenomenon occurring based on the macro-phenomenon.

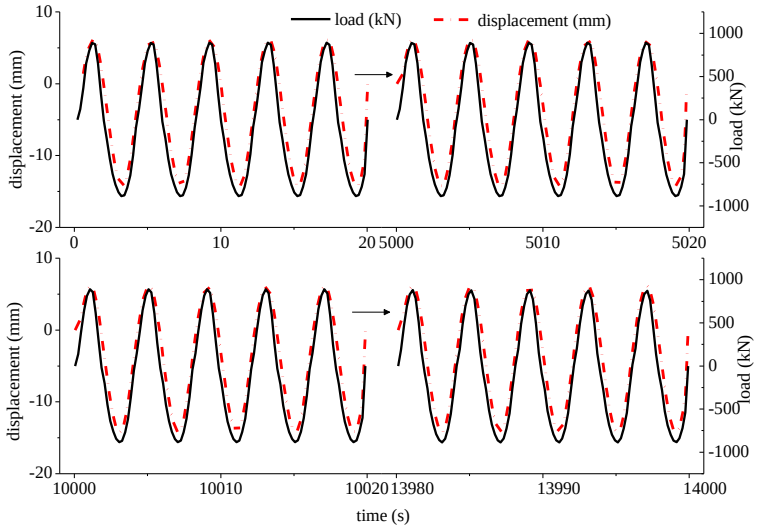

Figure 5. Typical shear failure.

3.3. Energy dissipation capacity

Based on the load-displacement data, the energy dissipation at different monitoring nodes could be obtained by numerical integration, and the changes of mechanical properties and the development of cumulative damage were observed through energy dissipation value.

Figure 6 shows the energy dissipation analysis of the corresponding monitoring points of the specimens. The results indicated that the energy dissipation values decreased slowly on the whole. That was because the micro cracks grew gradually in composite materials with the cumulative damage increasing constantly. Meanwhile, the specimens turned from elastic into elasto-plastic state. After the transcendental cumulative damage, the fatigue damage increased gradually. Though the load-displacement-time curve indicated that no apparent degradation phenomenon could be observed, the energy dissipation analysis revealed the slow cumulative fatigue damage process.

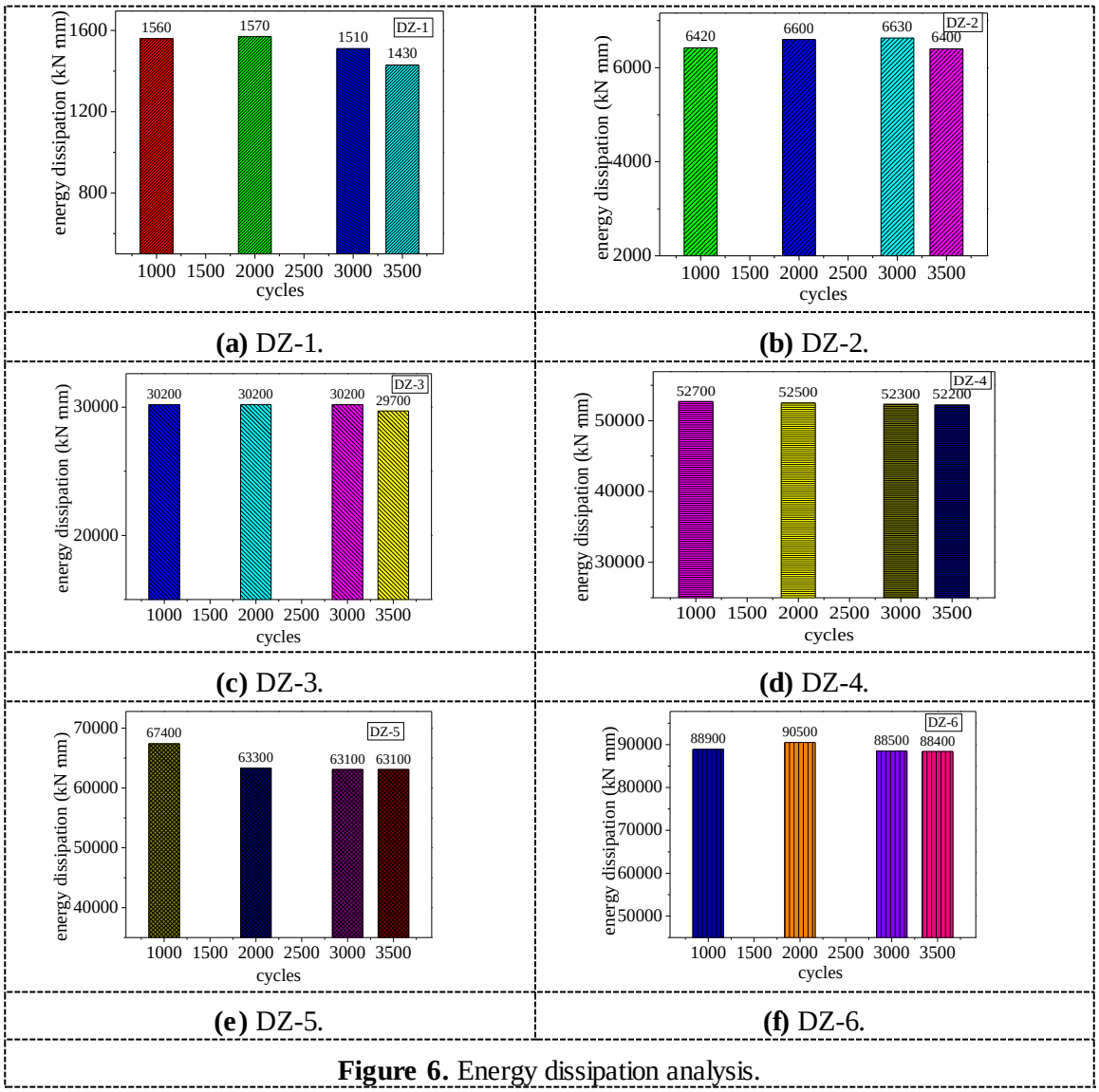

(a) DZ-1. **(b)** DZ-2.

(c) DZ-3. **(d)** DZ-4.

(e) DZ-5. **(f)** DZ-6.

Figure 6. Energy dissipation analysis.

3.4. Residual bearing capacity

After fatigue test, in order to guarantee the maximum safety margin, the axial compression test was carried out to derive the residual ultimate bearing capacity of DZ-5 and DZ-6 to investigate the negative effects under low-cycle fatigue loading. Figure 7 is the ultimate bearing capacity of the

specimens after fatigue test. The load-displacement curves were approximately linear before failure. Compared to the mean value 6472kN gained from same batch three specimens under axial compression test, it indicated that the relevant specimens undergoing 3500 cycles fatigue loading had an obvious decrease in ultimate bearing capacity. The residual bearing capacity of DZ-6 decreased at a most obvious extent 13.47% compared to DZ-5 with 6.5%. The residual bearing capacity can provide reference basis for cumulative damage evaluation and fatigue life prediction.

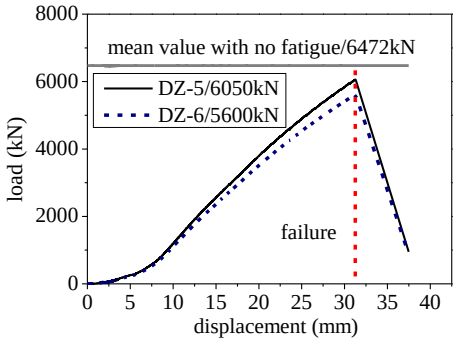

Figure 7. Analysis of the residual bearing capacity.

3.5. Fatigue life prediction based on the residual strength theory

The residual strength is one of the most important properties of composite materials after fatigue loading and is the basis of cumulative damage assessment and fatigue life prediction [12]. Considering the requirement that the parameters should be measured easily, it is assumed for the definition of cumulative damage model that the strength loss can be used as a metric to evaluate fatigue damage phenomenologically. In this part, the residual strength theory can be applied to assess the fatigue cumulative damage and predict fatigue life.

The residual ultimate bearing capacity of the specimens after fatigue test could be obtained in the form of axial compressive ultimate bearing capacity, and the residual strength $R(n)$ of specimens after nth loading cycle can be modified and expressed in Eq. (1) ~ Eq. (3) based on the existing theories [13-15]:

$$R(n) = R(0) - [R(0) - S_m] f(n / N_f) \tag{1}$$

$$f(n / N_f) = (\frac{n}{N_f})^V \tag{2}$$

$$V = \frac{E_{end}}{E_m} \tag{3}$$

where $R(0)$ is the ultimate bearing capacity with no fatigue; E_{end} is the energy dissipation value of the final cycle under fatigue loads; E_m is the maximum value of energy dissipation in fatigue loading history.

The cumulative damage can be determined as [13]:

$$\Delta D_n = A[R(n-1) - R(n)] \tag{4}$$

$$A = \frac{1}{R(0) - S_m} \tag{5}$$

where ΔD_n is the cumulative damage value after nth cycle; S_m is the peak fatigue load.

Table 3 gives the fatigue life prediction results and cumulative damage values based on the macroscopic residual bearing capacity of the specimens. Taking the average residual bearing capacity of DZ-5 and DZ-6 as the specimen JZ-7, the most unfavorable loading condition 6 was used to predict the mean fatigue life.

The fatigue life of DZ-6 specimen can reach up to 23372 cycles under the most unfavorable loading condition 6 and the average fatigue life predicted by the mean residual ultimate bearing capacity after fatigue is up to 33,243 cycles. The overall prediction result shows that the GFRP cross arms with steel sleeves demonstrate high level of safety redundancy on anti-fatigue performance.

Table 3. Fatigue life prediction.

Specimen	Degradation parameter V	Residual bearing capacity (kN)	Cumulative damage value	Fatigue life prediction
DZ-5	0.9362	6050	0.07337	57002
DZ-6	0.9768	5600	0.15650	23372
JZ-7	0.9565	5825	0.11612	33243

4. Conclusions

The conclusions can be drawn within the research scope:

1) Although the load-displacement-time curve shows that there was no apparent degradation phenomenon, the energy dissipation analysis revealed the slow cumulative fatigue damage process during low-cycle loading.
2) The GFRP cross arms with steel sleeves, experienced low-cycle fatigue loading, could display excellent elastic workability until the limit state of bearing capacity.
3) Based on the residual strength theory, the cumulative fatigue damage was evaluated and the fatigue life was predicted based on component level. Overall, the GFRP cross arms demonstrate high safety redundancy under different low-cycle fatigue loading, and can be expected for wide application in transmission towers.

Acknowledgement

The authors are grateful to everyone participating in this research for their assistance during the experimental program. This research is financially supported by the State Grid Corporation of China (SGTYHT/15-JS-197), and the support is gratefully acknowledged.

References

[1] Fujikake K, Mindess S and Xu H 2004 *J.Compos. Constr.* **8(4)** 341
[2] Savory E, Parke G A R, Zeinoddini M, Toy N and Disney P 2001 *Eng. Struct.* **23(4)** 365
[3] Momomura Y, Marukawa H, Okamura T, Hongo E and Ohkuma T 1997 *Wind Eng. Ind. Aerodyn.* **72** 241
[4] Hashin Z and Rotem A 1973 *J. Compos. Mater.* **7(4)** 448
[5] Hashin Z 1985 *Compos. Sci. & Technol.* **23(1)** 1
[6] Talreja R 1979 *Eng. Fracture Mech.* **11(4)** 839
[7] Yang J N, Lee L J and Sheu D Y 1992 *Compos. Struct.* **21(2)** 91
[8] Shokrieh M M and Taheri-Behrooz F 2006 *Compos. Struct.* **75(1-4)** 444
[9] Varvani-Farahani A, Haftchenari H and Panbechi M 2006 *J. Compos. Mater.* **40(18)** 1659
[10] Eliopoulos E N and Philippidis T P 2011 *Compos. Sci. & Technol.* **71(5)** 742
[11] Brunbauer J, Stadler H and Pinter G 2015 *Int. J. Fatigue* **70** 85
[12] Yang J N and Liu M D 1977 *J. Compos. Mater.* 11(2) 176
[13] Yao W X and Himmel N 2000 *Compos. Sci. & Technol.* **60(1)** 59
[14] Chou P C and Croman R 1978 *J. Compos. Mater.* **12(2)** 177
[15] Schaff J R and Davidson B D 1997 *J. Compos. Mater.* **31(2)** 128